ISIJ International, Vol. 35 (1995), No. 3, pp. 317–323

Improvement of Creep Rupture Strength of High Cr Ferritic Steel by Addition of W

Yutaka TSUCHIDA, Kentaro OKAMOTO[1] and Yoshikuni TOKUNAGA

Nagoya R & D Labs, Nippon Steel Corporation, Tokai, Tokai, Aichi-ken, 476 Japan.
1) Formerly Steel Research Laboratories, Nippon Steel Corporation. Now at Nippon Steel Metal Products Co., Ltd., Ginza, Chuo-ku, Tokyo, 104 Japan.

(Received on July 13, 1994; accepted in final form on December 16, 1994)

The effect of W addition on creep rupture strength (CRS) of high Cr ferritic steel was evaluated with three kinds of steels; base steel of 9Cr–1Mo–V–Nb–N, 0.7% W addition to base steel, and 1.7% W addition with decreased Mo addition to 0.5%. The latter two steels have the same values of Mo+0.5W *viz.* Mo equivalent. Further, the reasons for the beneficial effect of W was analyzed.

The CRS at 600°C for 1 000 h increases with W addition at a rate of 35 MPa/% W. As the hardness remains almost constant during the creep test, the enhancement of CRS could not be attributed to the formation of precipitate or cluster during the creep test. The W addition was found to increase the partition of Nb to VN, resulting in the lattice expansion of VN and enhancing the CRS through coherency strain around VN. This effect accounts for about half of the increase of CRS by W addition.

The W addition also causes the precipitation of a film-like Laves phase along the subgrain boundary. Inconsequently, Cr_2C precipitates simultaneously. The Laves phase contributes to the other half of the CRS increase, possibly through suppressing the growth of subgrain during the creep test.

KEY WORDS: 9Cr ferritic steel; creep rupture strength; W addition; NbN; VN; $M_{23}C_6$; globular Laves phase; film-like Laves phase; Cr_2C; coherency strain; subgrain size.

1. Introduction

High Cr ferritic steels, such as 9Cr–1Mo–V–Nb–N steel (Mod.9Cr–1Mo steel[1]), are comparable in creep rupture strength (CRS) to the austenitic stainless steels at 600°C. As these ferritic steels have higher thermal conductivity and smaller thermal expansion coefficient, they are less sensitive to the failure caused by thermal cycling. As a result, these steels are applied to the ultra supercritical boilers and other high temperature plants.[2–4]

Ultra supercritical boilers require enhanced steam conditions of increased pressure and elevated temperature in order to improve the power generating efficiency, and improved CRS of the materials is strongly desired. To meet the demand, several advanced types of 9 to 12% Cr steels have been developed with more than 1.5% W addition.[5–8] These new steels work at temperatures 20 to 25°C higher than that of Mod.9Cr–1Mo steel. Tungsten is also alloyed to the high Cr ferritic steels that are under development for the use in primary walls of fusion reactors.[9–11] Though the tungsten addition is useful for the improvement of CRS of high Cr ferritic steels, the reasons are not completely realized yet.

The authors have analyzed the governing factors of CRS of Mod.9Cr–1Mo steel and have pointed out the importance of inter-particle distance and size of VN, and the misfit of VN with matrix.[12–15] In this report, the role of VN in the W alloyed high Cr ferritic steels has been examined, and the unique effects of W in the steels have been analized. It also discusses the precipitation behavior that is specific for W alloying.

2. Experimental Procedure

Three types of 30 kgf ingots, whose compositions are listed in **Table 1**, were prepared by vacuum induction melting. Steel A is the base steel and has a composition equivalent to Mod.9Cr–1Mo steel. Steel B contains 0.7% W added to the base steel, while Steel C has the same Mo equivalent value (Mo+0.5W) as Steel B with W increased to 1.7% and Mo decreased to 0.5%.

Each of these ingots was heated to 1 250°C and was rolled into a 20 mm thick plate with a finish-rolling

Table 1. Chemical compositions of the steels examined. (mass%)

	C	Si	Mn	Cr	Mo	W	V	Nb	Al	N
A	0.10	0.05	0.42	9.1	0.90	—	0.24	0.041	0.01	0.031
B	0.11	0.05	0.18	8.4	0.99	0.71	0.15	0.041	0.01	0.031
C	0.10	0.05	0.19	8.8	0.49	1.76	0.15	0.056	0.01	0.035

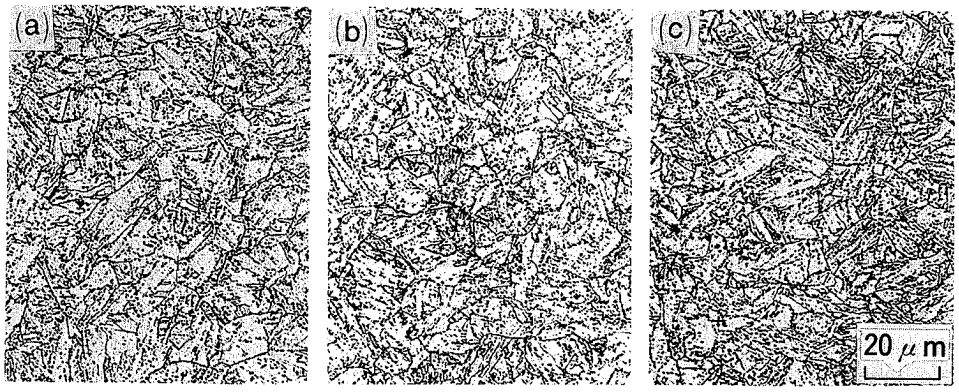

Fig. 1. Optical microphotographs after heat treatment.
(a) Steel, A, (b) Steel B, (c) Steel C

temperature of 1 000°C. Then the plate was air-cooled to room temperature and subjected to normalizing at 1 050°C for 1 h and somewhat longer tempering at 760°C for three hours that also served as post-weld heat treatment (PWHT). The tempering parameter T $(20+\log t)$ was as large as 21 200, where T is temperature (K) and t is time (h).

Round bar specimens, whose gauge section was 6 mm in diameter and 30 mm in length, were machined at the mid-thickness of the plates so that the longitudinal direction was perpendicular to the rolling direction (T direction). They were tested on multiple creep rupture testing machines at 600°C. The creep ruptured specimens were subjected to Vickers hardness measurement at the head of them according to the method of JIS Z2244.

For the tensile test, round bar specimens whose gauge section was 10 mm in diameter and 50 mm in length were machined at the mid-thickness of the plates so their longitudinal direction would be the T direction. Tensile tests were carried out at 550°C in accordance with JIS G0567.

Microstructural observation was conducted on the longitudinal section of the plate. Thin films and extraction replicas taken from gauge sections near the fracture surface were observed with transmission electron microscope (TEM) equipped with energy dispersive X-ray spectroscopy (EDS). Further, electrolytically extracted residue from the heads was chemically analyzed and the amount of elements in the precipitates were calculated as mass percent in the steel. The residue was also subjected to X-ray diffraction with Cu target.

3. Experimental Results

3.1. Microstructure

Figure 1 shows the microphotographs of the plates. All of them were tempered martensite without δ ferrite. Laves phase did not exist in all of them. The prior γ grain size of each plate was about 20 to 30 μm.

3.2. Creep Rupture Strength

Figure 2 shows the creep rupture test results of each plate, together with the average trend curves of those of Mod.9Cr–1Mo steel. It can be seen that CRS is improved by increased amount of W. **Figure 3** illustrates the 1 000 h CRS at 600 °C (σ_R) determined in Fig. 2 as a function

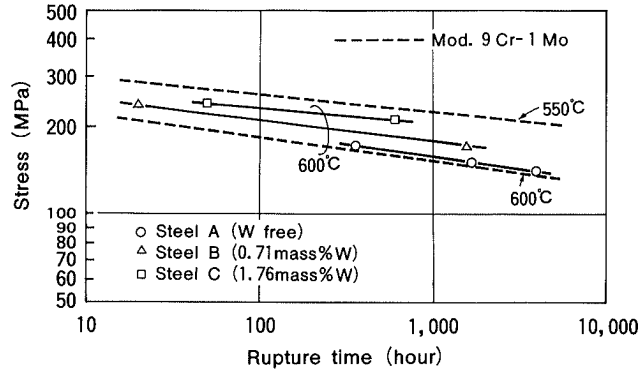

Fig. 2. Creep rupture curves for Steels A to C.

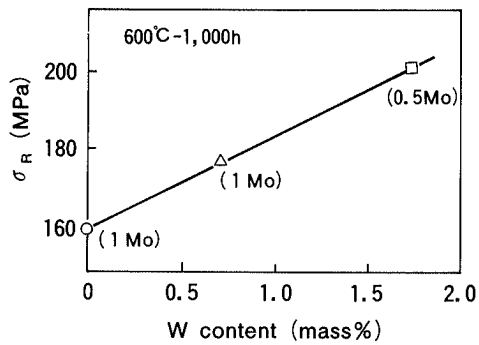

Fig. 3. Relation between creep rupture strength and the amount of W addition.

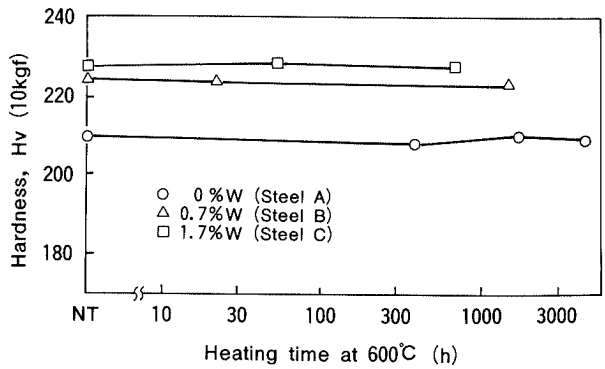

Fig. 4. Hardness change in the head of the creep ruptured specimens.

of W addition. As the amount of W addition increases, σ_R is increased at the rate of 35 MPa/%W. As far as the Mo content is in the range of 0.5 to 1 %, the effect

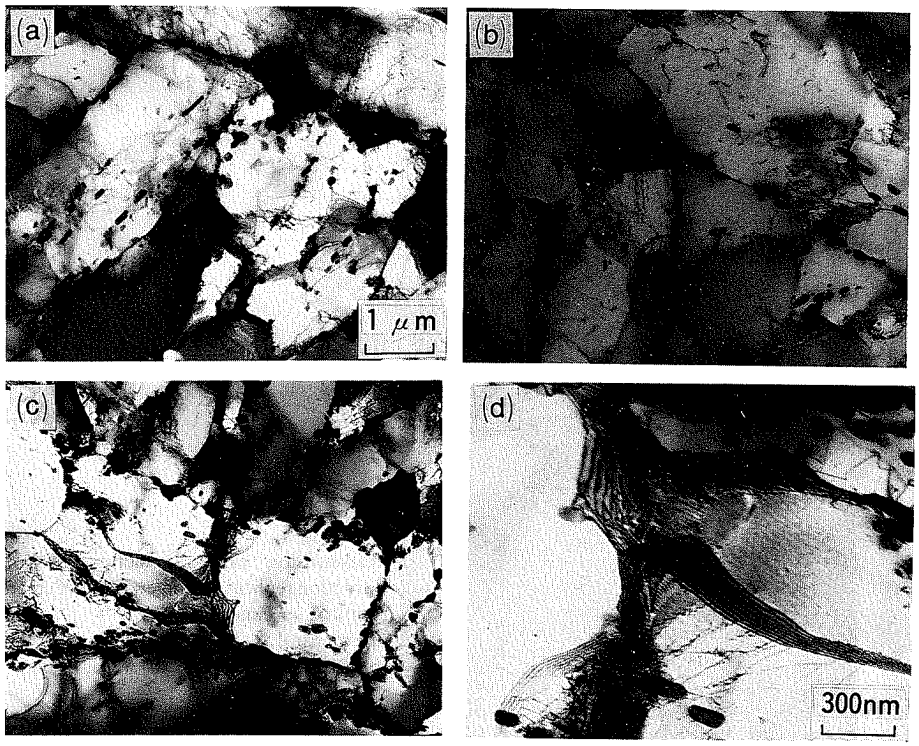

Fig. 5.
Transmission electron micrographs of Steels A to C at gauge sections of creep ruptured specimens.
(a) Steel A, 600°C, 147 MPa, 1 706 h
(b) Steel B, 600°C, 168 MPa, 1 449 h
(c), (d) Steel C, 600°C, 207 MPa, 669 h

of the amount of Mo is negligibly small.

The rupture elongation of each specimen was larger than 20%.

3.3. Hardness of Creep Specimens

Figure 4 shows the hardness change during creep test at 600 °C. The hardness of each steel remained almost unchanged.

3.4. Substructure

Figures 5(a) to **5(c)** show the electron microphotographs of gauge sections near the fracture surfaces of the creep ruptured specimens. Growth of subgrain is notable in Figs. 5(a) and 5(b). Massive precipitates were observed along prior γ grain and subgrain boundaries (hereafter simply called grain boundaries). The amount of precipitates was increased with increased addition of W.

In Steels A and B whose W contents are equal to or less than 0.71%, massive precipitate was also recognized within the subgrain. This indicates that the boundary moved beyond the martensite lath boundary and the subgrain grew in size. On the other hand, in Steel C that contains 1.76% W, the subgrain size is obviously smaller than those of Steels A and B. The grain boundaries in Steel C, as shown in **Fig. 5(d)**, were deflected in a complicated manner, suggesting that the growth of subgrain is restrained by precipitates along grain boundaries.

3.5. X-ray Diffraction of Extracted Residue

Figure 6 shows the results of X-ray diffraction of extracted residue. As the amount of W is increased, the shoulders of (511) and (422) diffraction peaks of $M_{23}C_6$ increased. The shoulder on the larger diffraction angle side of (511) diffraction peak is considered owing to Laves phase (Fe_2W). Since no marked peak was observed in the shoulder, it is estimated that W in Laves phase is

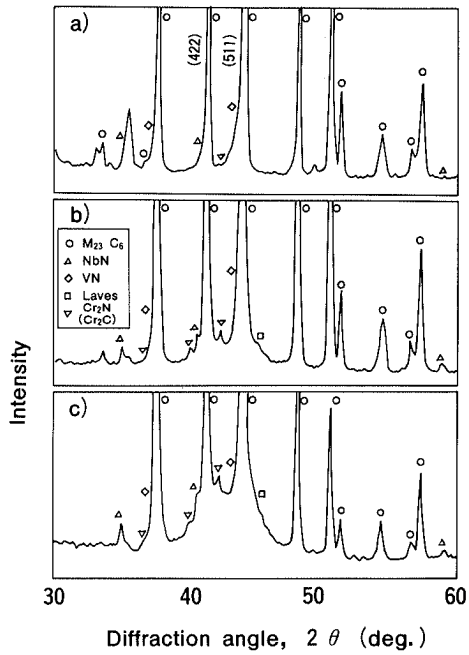

Fig. 6. X-ray diffraction of extracted residue from the head of creep ruptured specimens.
(a) Steel A, 600°C, 147 MPa, 1 706 h; (b) Steel B, 600°C, 168 MPa, 1 449 h; (c) Steel C, 600°C, 207 MPa, 669 h

irregularly substituted by Cr, Mo and others, causing its lattice constant to be widely scattered. The shoulder of (422) diffraction peak of $M_{23}C_6$ is considered due to the diffraction of Cr_2X (either Cr_2N or Cr_2C).

3.6. Precipitates along Grain Boundary

Figure 7 shows TEM images of extraction replicas prepared in the vicinity of the fracture. A comparison of Figs. 7(a) and 7(b) shows that the W addition enhances the precipitation along grain boundaries. Electron beam diffraction and EDS reveal that the precipitates along

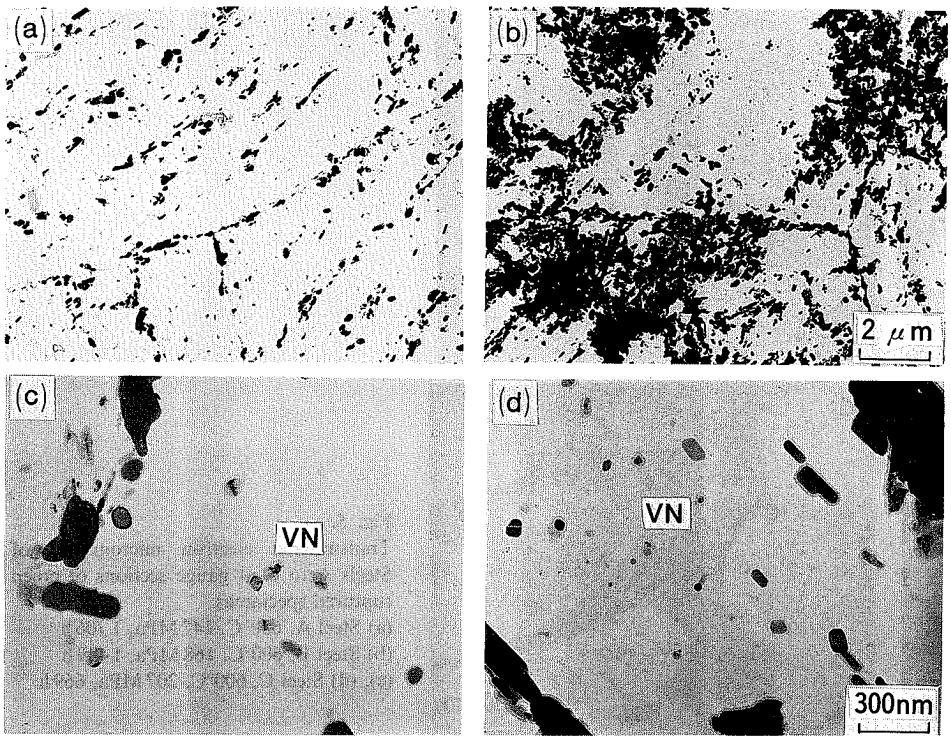

Fig. 7.
Transmission electron micrographs of extraction replicas at gauge section of creep ruptured specimens.
(a), (c) Steel A, 600 °C, 147 MPa, 1 706 h
(b), (d) Steel B, 600°C, 207 MPa, 601 h

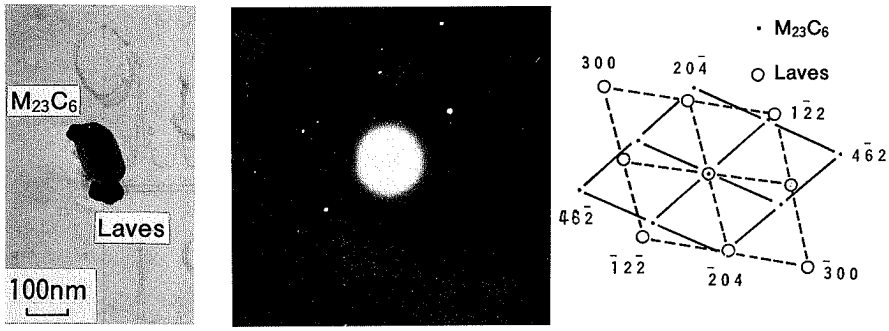

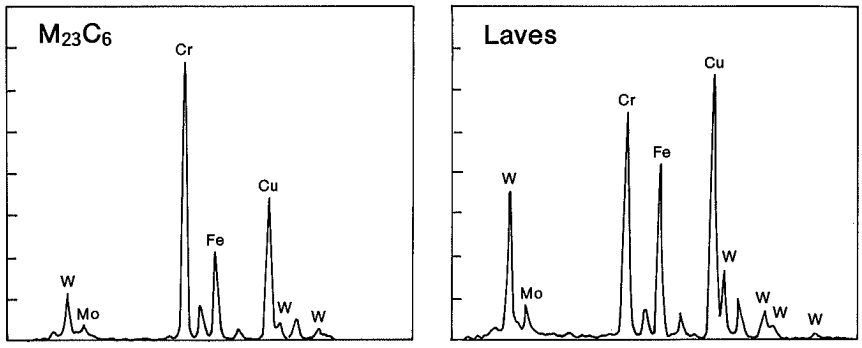

Fig. 8.
In situ formation of Laves phase at $M_{23}C_6$ in 1.76 mass% W containing steel (Steel C).

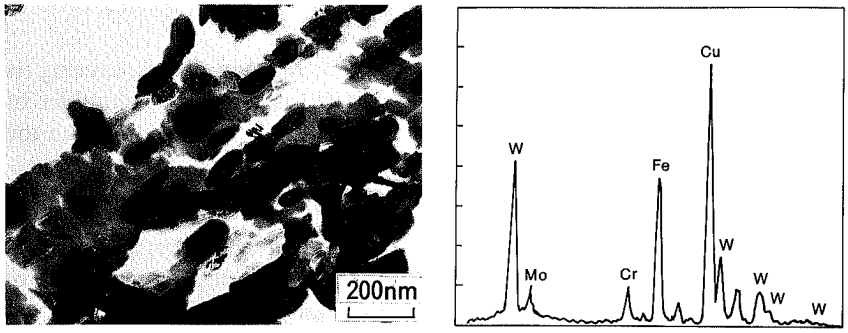

Fig. 9.
TEM image and EDS spectrum of film-like precipitates among grain boundary massive precipitates in the creep ruptured specimen of Steel C.

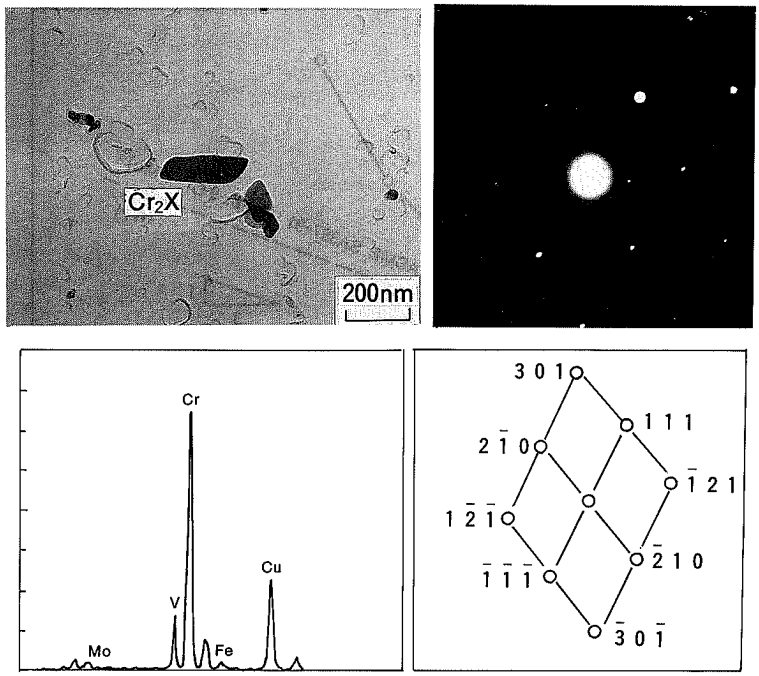

Fig. 10.
EDS spectrum and electron diffraction pattern of Cr_2X (Cr_2C or Cr_2N) in Steel C.

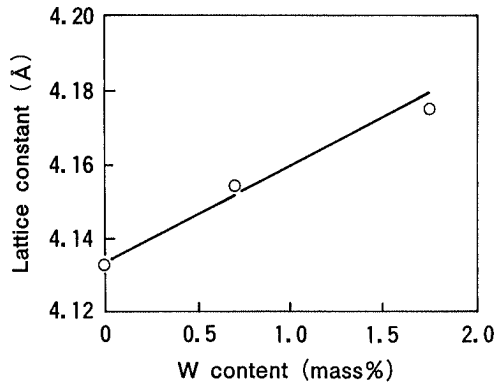

Fig. 11. Expansion of VN lattice constant with addition of W.

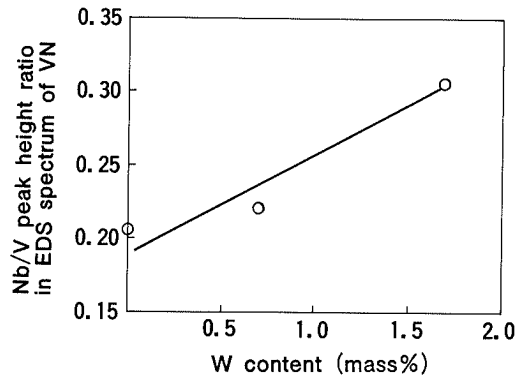

Fig. 12. Change of Nb/V peak height ratio in EDS spectrum of VN with W addition.

those boundaries mainly consist of massive $M_{23}C_6$. As shown in **Fig. 8**, some $M_{23}C_6$ were observed in combination with the granular Laves phase. Further, the massive $M_{23}C_6$ and the combined precipitates of $M_{23}C_6$ and Laves phase are connected with each other by the film-like substance that is shown in **Fig. 9**. From the result of EDS analysis which is also shown in Fig. 9, the substance is estimated to be the Laves phase. It is considered that by the appearance of the film-like substance the massive precipitate along boundary fell in clusters on the replica film. Extraction replica in **Fig. 10** also proves the existence of Cr_2X (either Cr_2N or Cr_2C) that was expected by the X-ray diffraction of Fig. 6.

3.7. Fine Precipitates in Matrix

As shown in Figs. 7(c) and 7(d), thin plate-like VN that measures 100 to 150 nm in size is recognized in matrix. Though the size of VN is almost unaffected by the addition of W, the lattice constant of VN is increased by the addition of W as shown in **Fig. 11**. **Figure 12** shows the Nb to V peak height ratio (Nb/V ratio) in EDS spectrum of VN, and the Nb/V ratio is higher as the W addition is increased.

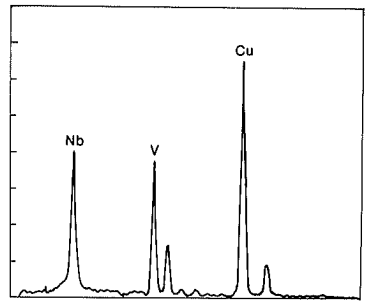

Fig. 13. EDS spectrum of NbN in Steel C.

Increased addition of W, in turn, makes the V solution into NbN increased. As a result, the peak heights of V and Nb become nearly the same, as shown in **Fig. 13** that is obtained from NbN in Steel C.

4. Discussion

4.1. Change of $M_{23}C_6$ during Creep Test

As the results of X-ray diffraction in Fig. 6 indicate, the addition of W causes the precipitation of Laves phase. The Laves phase exists either combined with $M_{23}C_6$ or

in film-like substance which connects $M_{23}C_6$ along the grain boundaries. Therefore, it is very likely that the Laves phase is formed from $M_{23}C_6$ during creep test.

Comparing the EDS spectra of $M_{23}C_6$ and Laves phase in Fig. 8, it can be seen that exclusion of Cr and condensation of W in $M_{23}C_6$ make up the composition of Laves phase. As the Laves phase is an inter-metallic compound, which does not contain C, the following reaction can be derived for the formation of Laves phase from $M_{23}C_6$.

$$p(\mathrm{Cr, Fe, Mo, W})_{23}C_6 + q\underline{\mathrm{W}} = s(\mathrm{Fe, Cr})_2(\mathrm{W, Mo}) + t(\mathrm{Cr\ carbide}) \quad \text{.....(1)}$$

where, p, q, s and t are constants and $\underline{\mathrm{W}}$ is W in matrix.

Figures 6 and 9 demonstrate the existence of precipitate which is identified as either Cr_2N or Cr_2C. Since the steels contain large amount of Nb and V which are stronger nitride formers than CrN, N is supposed to be mostly fixed as stable nitrides; Cr_2N is estimated to be difficult to exist. Further, Cr carbides could be formed together with Laves phase according to Eq. (1), the precipitates recognized in Fig. 6 or 9 are considered to be Cr_2C.

4.2. Change in VN Caused by W Addition

As shown in Fig. 11, the lattice constant of VN is increased by W addition. At the same time, Nb solution into VN is also increased as shown in Fig. 12. As described in the previous report,[13] the increased solution of Nb into VN makes the VN lattice expand. Thus, the expansion of lattice constant in Fig. 11 should be ascribed to the enhanced solution of Nb into VN by W addition.

As shown in Fig. 13, NbN of W alloyed steel contains a large amount of V. Combining the results illustrated in Figs. 12 and 13, it may be concluded that W addition enhances the mutual solution of VN and NbN and results in smaller difference in nature among them. The reason for this is a problem to be clarified.

4.3. Improvement of Creep Rupture Strength by W Addition

In the previous report,[12] CRS of 9Cr–1Mo–V–Nb–N steel has been analyzed in different conditions of heat treatment, and it has been shown that the increase of CRS ($\Delta\sigma_R$) varies approximately in accordance with the following equation,

$$\Delta\sigma_R \fallingdotseq 1/3\Delta\sigma_y \quad \text{.....(2)}$$

due to the change of inter-precipitate distance (λ), where $\Delta\sigma_y$ is the increase in 0.2% proof strength at 550°C. Besides, it has also been considered that $\Delta\sigma_R$ can be increased by both the increases of VN size and the coherency strain between VN and matrix.

Figure 14 shows the relation between σ_R and σ_y, when the amount of W addition is varied. The inclination between σ_R and σ_y in Fig. 14 is higher than 0.5; $\Delta\sigma_R$ cannot be explained solely by Eq. (2). As shown in Fig. 7, the size of VN hardly changes with W addition. Therefore, the coherency strain between VN and matrix, that is controled by the lattice constant of VN, is also considered to influence σ_R.

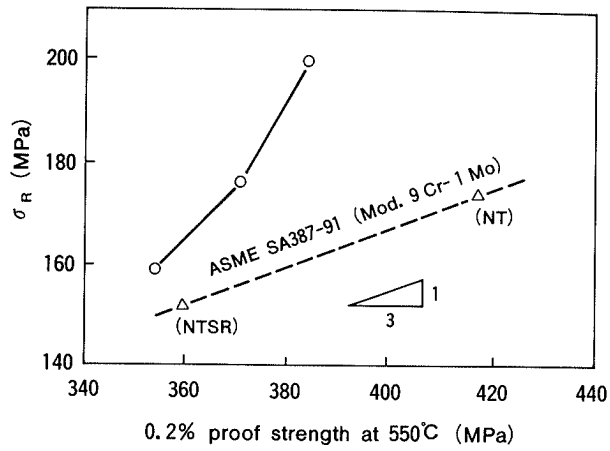

Fig. 14. Relation between 600°C–1 000 h rupture strength and 0.2% proof strength at 550 °C in the steels examined.

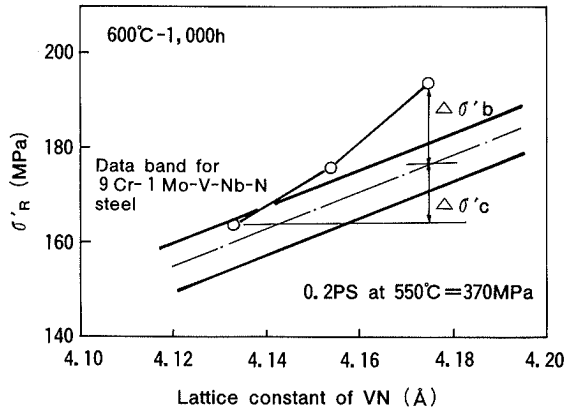

Fig. 15. Contribution of lattice constant of VN to the creep rupture strength of W alloyed steels.

For the purpose of evaluating σ_R under constant λ, σ_R at σ_y of 370 MPa, which can be called proof strength compensated CRS at 600°C for 1 000 h (σ'_R), was obtained in Fig. 14, using the inclination of 1/3. σ_y of 370 MPa was selected because it is almost the average σ_y of the steels examined. **Figure 15** shows the relation between σ'_R of the present steels and that of 9Cr–1Mo–V–Nb–N steel in the previous reports,[13-14] and the lattice constant of VN. Though σ'_R of the base steel without W addition (Steel A) falls within the data band of previous 9Cr–1Mo–V–Nb–N steel, σ'_R of Steels B and C which contains 0.71% W and 1.76% W respectively fall above the data band.

Regarding that the center of the data band of 9Cr–1Mo–V–Nb–N steel represents the upper limit of $\Delta\sigma'_C$, the increase of σ'_R by the change of lattice constant of VN, the increase of $\Delta\sigma'_C$ only accounts for about half of the measured increase. The rest of the increase of CRS, $\Delta\sigma'_b$, which is equivalent to a ten-fold increase with respect to rupture time, is considered to be governed by factors which are specific to W addition. In the following, the factors will be discussed.

Solid-solution strengthening of W is often considered as the factor for improvement of CRS in the W alloyed steels. The atomic size of W is 2.741 A[16]; only 0.6% larger than 2.725 A[16] of Mo. Besides, the amount of solute W in matrix decreases[17] markedly during a creep

test. The marked effect of W on CRS over Mo could not be explained in terms of solid-solution strengthening.

If fine precipitation or clustering was caused by W addition during a creep test, it might improve the CRS of the steel. Though such precipitate or cluster should influence the strength and hardness, the hardness of the creep ruptured specimens is almost constant as is shown in Fig. 5, indicating that the increase of CRS by W addition is not attributed to the fine precipitation or clustering. As discussed before, Cr_2C can precipitates together with Laves phase formation from $M_{23}C_6$. It is estimated to be ineffective on strengthening for the above mentioned reason.

As shown in Figs. 8 and 9, W addition enhanced the formation of Laves phase which precipitates in connection with massive $M_{23}C_6$ or the formation of film-like Laves phase. These phases, as shown in Fig. 5(d), impede the movement of subgrain boundaries.

The creep deformation rate ($\dot{\varepsilon}$) is not only dependent on the precipitation of VN in matrix, but also dependent on third power of subgrain size according to Sherby *et al.*[18] In the present study, as shown in Fig. 5, the subgrain size of 1.7% W containing steel is about half of that of the steel without W addition and this makes $\dot{\varepsilon}$ reduced to one-eighth. Applying the following Monkman-Grant rule to the relationship between minimum creep rate ($\dot{\varepsilon}_m$) and creep rupture time (t_R)

$$\dot{\varepsilon}_m \cdot t_R = \text{const} \quad \text{.....(3)}$$

and assuming $\dot{\varepsilon}_m$ as $\dot{\varepsilon}$, t_R becomes eight-fold. This increase of t_R corresponds roughly to the aforementioned increase of creep rupture time that is specific to W addition.

5. Conclusions

Using 9Cr ferritic steels with various amounts of W, the role of W addition for creep rupture strength (CRS) has been analyzed. The following points have been clarified.

(1) The CRS increases linearly with W addition, but is independent on Mo equivalent (Mo + 0.5 W).

(2) The hardness remains almost unaffected during creep tests, indicating the improvement of CRS is not attributed to the fine precipitation or clustering.

(3) The addition of W enhances the partition of Nb into VN, and causes the increase of the lattice constant of VN.

(4) In steel with W addition, granular or film-like Laves phases are formed from massive $M_{23}C_6$ along grain boundaries during creep test. This reaction forms Cr_2C as well.

(5) W addition increases CRS at 600°C for 1000 h at the rate of 35 MPa/%W. About one-half of the increase is due to the enhanced solution of Nb into VN. The remaining half is considered to be due to the restraint of subgrain growth by film-like Laves phase along γ grain boundary and subgrain boundary.

REFERENCES

1) V. K. Sikka: Proc. Topical Conf. on Ferritic Alloys for Use in Nuclear Energy Technologies, Snowbird, Utah, (June 1983), 317.
2) F. Masuyama, T. Hada, S. Kaneko and R. Toyoda: *Mitsubishi Heavy Ind. Tech. Rep.*, **24** (1987), 491.
3) H. Umaki, I. Kajiki, T. Kunihiro, T. Tozuka, M. Nakadai and R. Kume: *IHI Technical Report*, **31** (1991), 339.
4) I. Nihei: 133th Nishiyama Memorial Seminar, ISIJ, Tokyo, (1990), 211.
5) T. Fijita: *ISIJ Int.*, **32** (1992), 175.
6) H. Naoi, H. Mimura, M. Ogami, M. Sakakibara, S. Araki, Y. Sogou, T. Ogawa, H. Sakurai and T. Fujita: *Nippon Steel Tech. Rep.*, (1992), No. 347, 27.
7) A. Iseda, H. Teranishi, K. Yoshikawa, F. Masuyama, T. Daikoku and T. Hada: *Fossile Atomic Power Generation*, **39** (1988), 897.
8) A. Iseda, Y. Sawaragi and F. Masuyama: *CAMP-ISIJ*, **4** (1991), 1991.
9) F. Abe, T. Noda and M. Okada: *J. Nucl. Mater.*, **195** (1992), 51.
10) M. Tamura, H. Hayakawa, M. Tanimura, A. Hishinuma and T. Kondo: *J. Nucl. Mater.*, **141/143** (1986), 1067.
11) E. Dequidt, J. Arroyo and M. Schirra: *J. Nucl. Mater.*, **179/181** (1991), 659.
12) Y. Tsuchida, T. Takeda and Y. Tokunaga: *Tetsu-to-Hagané*, **80** (1994), 723.
13) Y. Tsuchida, K. Okamoto and Y. Tokunaga: to be published *Tetsu-to-Hagané*.
14) Y. Tsuchida, K. Tokuno, K. Okamoto and Y. Tokunaga: *ISIJ Int.*, **35** (1995), 309.
15) Y. Tsuchida, H. Sakurai, K. Okamoto and Y. Tokunaga: to be published in *J. Welding Inst. Jpn.*
16) Rikagaku-Jiten (Dictionary for Physics and Chemisty), Iwanami Shoten, Tokyo, (1986).
17) K. Tokuno, K. Hamada and T. Takeda: *CAMP-ISIJ*, **3** (1990), 837.
18) O. D. Sherby, R. H. Klundt and A. K. Miller: *Metall. Trans.*, **6A** (1977), 843.